Heliyon 9 (2023) e22876

Contents lists available at ScienceDirect

Heliyon

journal homepage: www.cell.com/heliyon

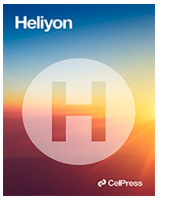

Magnetic properties of Fe-doped NiO nanoparticles

Alex Soares de Brito [a], Marlon Ivan Valerio-Cuadros [a,b], Lilian Felipe Silva Tupan [a,c], Aline Alves Oliveira [a], Reginaldo Barco [a], Flávio Francisco Ivashita [a], Edson Caetano Passamani [d], José Humberto de Araújo [e], Marco Antonio Morales Torres [e], Andrea Paesano Jr. [a,e,*]

[a] Departamento de Física, Universidade Estadual de Maringá, Av. Colombo, 5790, Jardim Universitário, 87020-900, Maringá, PR, Brazil
[b] Facultad de Ciencias Físicas, Universidad Nacional Mayor de San Marcos, Lima, Peru
[c] Centro Universitário Ingá, 87035-510, Maringá, PR, Brazil
[d] Departamento de Física, Universidade Federal do Espírito Santo, 29075-910, Vitória, ES, Brazil
[e] Departamento de Física Teórica e Experimental, Universidade Federal do Rio Grande do Norte, 59078-970, Natal, RN, Brazil

ARTICLE INFO

Keywords:
Nanoparticles
Nickel oxide
Fe-doped
Core-shell model
Spin-glass
Cluster-glass

ABSTRACT

Undoped and Fe-doped NiO nanoparticles were successfully synthesized using a lyophilization method and systematically characterized through magnetization techniques over a wide temperature range, with varying intensity and frequency of the applied magnetic fields. The $Ni_{1-x}Fe_xO$ nanoparticles can be described by a core-shell model, which reveals that Fe doping enhances exchange interactions in correlation with nanoparticle size reduction. The nanoparticles exhibit a superparamagnetic blocking transition, primarily attributed to their cores, at temperatures ranging from above room temperature to low temperatures, depending on the Fe-doping level and sample synthesis temperature. The nanoparticle shells also exhibit a transition at low temperatures, in this case to a cluster-glass-like state, caused by the dipolar magnetic interactions between the net magnetic moments of the clusters. Their freezing temperature shifts to higher temperatures as the Fe-doping level increases. The existence of an exchange bias interaction was observed, thus validating the core-shell model proposed.

1. Introduction

Nanoparticles (NPs) have been intensively investigated in the last decades, particularly with respect to their striking structural, colloidal, adsorption and magnetic properties. NPs still constitute a rich system from the basic physics point of view and because of their potentials for different technological applications [1–4]. In the field of magnetism of NPs, several issues deserve to be elucidated, for instance, the finite-size effect that results in a net magnetic moment due to the symmetry breaking, at least, in antiferromagnets. Therefore, one of the most interesting NP systems are those synthesized from antiferromagnetic (AFM) materials which, in despite of

* Corresponding author. Departamento de Física, Universidade Estadual de Maringá, Av. Colombo, 5790, Jardim Universitário, 87020-900, Maringá, PR, Brazil.
E-mail addresses: alexsoaresdebrito@gmail.com (A.S. de Brito), marlon190@gmail.com (M.I. Valerio-Cuadros), lilian.tupan@hotmail.com (L.F. Silva Tupan), alineuem@hotmail.com (A.A. Oliveira), r_barco@hotmail.com (R. Barco), fivashita@gmail.com (F.F. Ivashita), passamaniec@yahoo.com.br (E.C. Passamani), humberto@fisica.ufrn.br (J. Humberto de Araújo), morales@fisica.ufrn.br (M.A. Morales Torres), apjunior@uem.br (A. Paesano).

https://doi.org/10.1016/j.heliyon.2023.e22876
Received 21 July 2023; Received in revised form 16 October 2023; Accepted 22 November 2023
Available online 28 November 2023

this magnetic order, may present a net magnetic moment due to the uncompensated spins at the NP surfaces, as previously established by Louis Néel in the earlies 60's [5,6].

Néel studied antiferromagnetic NiO NPs pointing for a superparamagnetic (SPM)-like behavior by which the net magnetic moments of single magnetic domains flip between two stable orientations, antiparallel to each other, separated by an energy barrier, $K.V = E_B$ (where K is the magnetic anisotropy constant and V the magnetic particle volume). The stable orientations define the magnetic easy axis of a magnetic NP. At a finite temperature, there is a finite probability for the magnetization to flip and reverse its direction in time. The mean time between two consecutive flips is called the Néel relaxation time τ_N. For non-interacting magnetic NPs, it is given by the Néel-Arrhenius equation, shown below:

$$\tau_N = \tau_0 \exp\left(\frac{KV}{k_B T}\right) \quad [1]$$

where k_B is the Boltzmann constant, T the temperature, and their product the thermal energy; τ_0 is a time characteristic of the material, called the *attempt time*, with typical values between 10^{-9} and 10^{-13} s.

Kodama et al. [7] also contributed to a fundamental understanding of this type of system and showed that the moments of NiO NPs are too large to be explained by a two-magnetic-sublattice model. Their observations were consistent with multi-sublattice spin configurations considering low coordination at the surface sites [7,8].

There are currently many works published on NiO NPs. There are also excellent reviews on this nanostructured system [1–3,9–14]. Therefore, it is not the purpose of this paper to comment on or complement them. However, one point we want to consider. According to the vast collection of experimental data published on this system it is observed that different NP synthesis processes can lead to distinct magnetic properties. The analysis conducted here (Section 3) is based on some prior work, particularly those that have revealed similarity with our experimental results.

A good strategy to better understand the NPs behavior is to place a marker or dopant that can probe some of their peculiar properties. Of course, the doping process may change the structure and magnetic properties of the starting systems, but this eventual effect may reveal new insights about nanomagnetic phenomena on the studied systems.

In this sense, the aim of this work was to investigate the effect of Fe doping in NiO nanoparticles synthesized by freeze-drying an aqueous solid solution of nickel and iron acetates followed by heat treatment under ambient atmosphere. This synthesis process has long been applied in our laboratory to prepare samples of diluted magnetic semiconductors and is described in detail elsewhere [15,16]. It has the advantage of producing samples with very precise total chemical composition and good tuning of NPs size through control of heat treatment temperature (although with some size distribution).

Some earlier studies were dedicated to Fe-doped NiO NPs [2,9,12,17–19] and to Fe-doped bulk NiO [20,21]. However, the nanostructured system lacks a more extensive magnetic characterization, thus leaving the description of the system incomplete under variation of both the doping level and the synthesis temperature. These two conditions may affect the crystallite sizes and consequently the exchange interactions in the NPs.

Thus, to achieve a more complete understanding of this nanostructured system we prepared $Ni_{1-x}Fe_xO$ NPs (with $x \leq 0.05$) at different synthesis temperatures. The samples were previously characterized by X-ray diffraction (XRD), transmission electron microscopy (TEM), Fourier transform infrared spectroscopy, and UV-VIS diffuse reflectance spectroscopy [22]. ^{57}Fe Mössbauer spectroscopy studies were also performed to finely detect iron containing phases (see a pair of representative Mössbauer spectra in Supplementary Material); full results from this nuclear characterization technique will be published elsewhere.

We report here the magnetic properties of the $Ni_{1-x}Fe_xO$ NPs obtained from direct current (DC) and alternating current (AC) magnetization techniques while varying the temperature measurements and the frequency of the field oscillation (for AC susceptibility). The static and dynamic magnetic analyses applied here allowed us to better understand the role of the finite size effect in the undoped or Fe-doped NiO nanoparticles and describe the influence at the doping level.

2. Materials and methods

The $Ni_{1-x}Fe_xO$ NPs characterized in this work were synthesized by freeze-drying and heat-treatments at 600 °C, 500 °C and 400 °C (see Supplementary Material for details on the preparation of these NPs). Only samples identified as monophasic were considered in the present study (i.e., $x \leq 0.04$). According to previous results obtained from the XRD and TEM analysis, the NPs exhibited approximately spherical or polyhedral shapes [22]. Iron doping induced minor changes in the lattice parameters, but a significant reduction in crystallite size and particle size (see Supplementary Material for respective methodological details).

The DC magnetic characterizations were performed in a SQUID-VSM magnetometer (Quantum Design/MPMS 3). The M(T) and M(H) curves were measured for all $Ni_{1-x}Fe_xO$ samples. M(T) curves were obtained applying zero-field cooling/field cooling (ZFC/FC) protocols, under probe fields H = 50, 500 and 5000 Oe. The M(H) curves were recorded at 2 K and 300 K (room temperature – RT). To investigate the presence of the exchange-bias effect, M(H) curves were also obtained in the FC protocol at 2 K after the sample has been cooled down from 300 K under applied field H = 70 kOe. The AC magnetization measurements were performed in an PPMS (Quantum Design/EverCool II). An AC test magnetic field of 10 Oe was used. The field oscillation frequency was varied from 50 to 10,000 Hz.

3. Results and discussion

The M(T) curves for the undoped sample are shown in Fig. 1. The curves are like others reported earlier for NiO NPs synthesized by

diverse methods [9,12,23,24]. In a partial concordance with these authors, the broad peak shown in the ZFC curve is attributed to a progressive blocking of the SPM cores where the peak broadening is an effect mainly associated with the particle size distribution of the NPs [9,12,]. In this sense, larger cores magnetically block near or just below RT, particles with medium sizes around T_1 (=122 K) and the smallest ones below T_1 as indicated by arrows in this figure. However, there is no reason to exclude the NPs shell of this blocking process. Despite its supposedly minor thickness, it is plausible to realize the shell as being formed by small regions with net magnetic moments, or SPM clusters, which are also blocked magnetically at the lowest temperatures.

To evaluate the anisotropy constant (K) of these NiO NPs (average diameter = 22.2 nm) using Equation (1) (with $\tau_N = 10$ s, $\tau_0 = 10^{10}$ s and $T = T_1$), we considered the magnetic energy barrier (K.V), where V is the average particle volume (see Table S1, in Supplementary Material, to find average volumes of all prepared NPs and some magnetic parameters obtained in this work). The estimation resulted in K = 7347 J/m^3, a value close to that usually determined for bulk NiO (i.e., 8000 J/m^3).

The sharp peak at T_2 (=10 K) could conceivably be related to the freezing of magnetic moments present in the shell, configuring a transition to a spin-glass (SG)-like state as proposed by Winkler et al. [14], or, more properly, due to a cluster-glass-like state established among the clusters composing the shell.

The changes in the M(T) curves due to the increasing applied magnetic field are seen in Fig. 1b and c. The broad peak is displaced at lower temperatures, and this is consistent with a blocking process of SPM domains. The sharpest peak also shifted to lower temperatures because of the increasing field.

In all pairs of M(T) curves, that related to the FC protocol increases monotonically and is not yet magnetically saturated at the lowest measurement temperature. This observation is an indirect signature of a SG-like state as also suggested by the ZFC M(T) curves. In addition, the high irreversibility temperature indicates the existence of interparticle magnetic interactions as frequently observed for an ensemble of concentrated NPs [25].

Fig. 2 shows the AC susceptibility curves (i.e., χ' *vs.* T) of the undoped NiO sample obtained at different frequencies. The χ' curves reveal (i) broad peaks for the temperature range above 60 K (centered at ~235 K), (ii) low-intensity peaks positioned at 47 K that are independent of frequency, and (iii) sharp peaks at lower temperatures that show frequency-dependent behavior, i.e., they shift to higher temperatures when the frequency increases. The broad peak can be related to the SPM blocking regime of NiO NPs, thus confirming the evidence offered by the DC M(T) measurements.

The low intensity and frequency independent peak characteristic of an AFM transition (this contribution is not clearly seen in M(T)

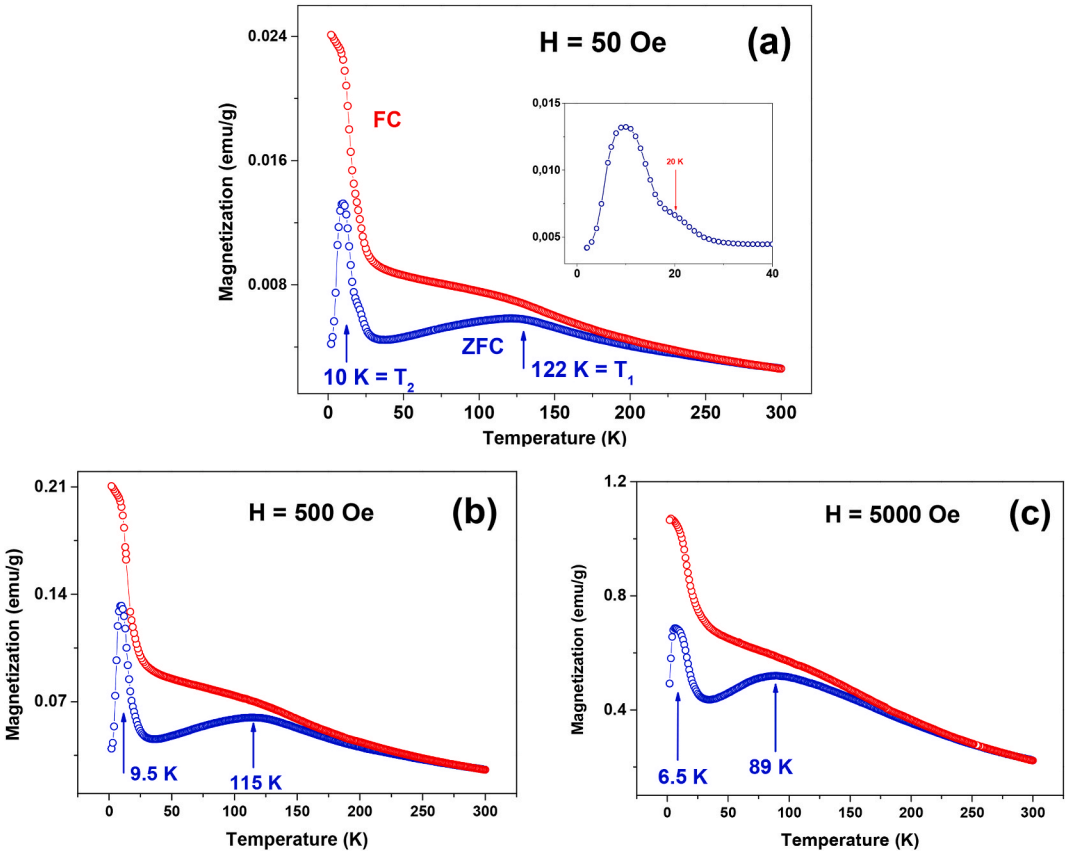

Fig. 1. M(T) curves of the undoped NiO sample (ZFC (blue) and FC (red) protocols) obtained for different probe fields: (a) H = 50 Oe; the insert shows an expanded view of the 2–40 K range; (b) H = 500 Oe; and (c) H = 5000 Oe.

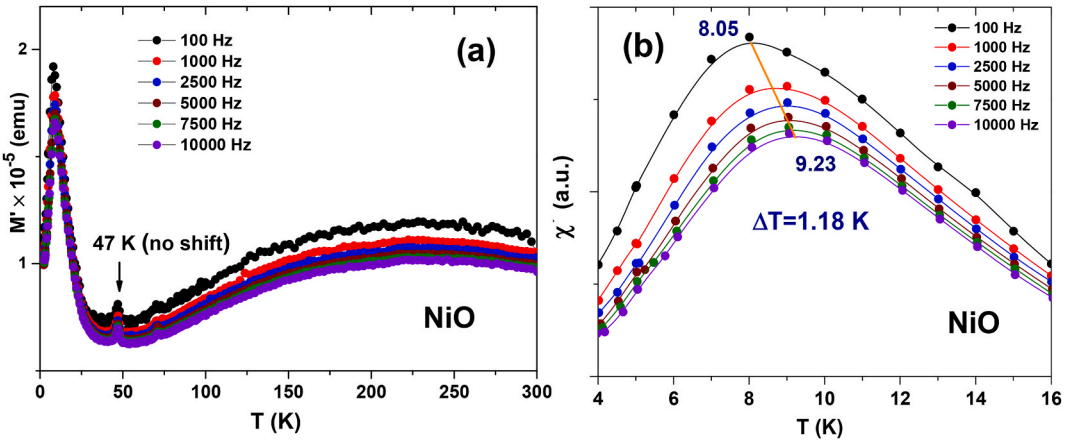

Fig. 2. χ(T) curves of the undoped NiO sample obtained for different frequencies f_{AC} (a); expanded view of the 4–16 K range where the continuous solid lines are spline fits (b).

data) and could be attributed to a small amount of air enclosed within the measuring ampoule. It is well known that O_2 has an AFM transition at ~50 K [26]. A similar set of peaks, though not so sharp and centered at 56 K, was identified by Tadic et al. [2]. High intensity and sharp peaks are seen at the lowest temperature range. These both decrease in height and shift to higher temperatures with increasing frequency (see also Fig. 2b). This peak was also detected by Tadic et al. [2] and may point either to a blocking of SPM domains or to a SG-like transition of already magnetically blocked domains as considered by Winkler et al. [14].

To better define the nature of this transition, the *first empirical parameter* $C_1 = \Delta T_f/(T_f \Delta \log f)$ [2,27] was calculated and resulted in a value of 0.068(4), a value close to that found by Tadic et al. (i.e., $C_1 = 0.08$) for their NiO NPs. C1 is >0.13 for non-interacting particles, $0.08 < C1 < 0.13$ for intermediate interactions, and $0.005 < C1 < 0.08$ for SG-like systems [27,28] (i.e., the first empirical parameter decreases with increasing strength of interparticle interactions [29]). Thus, we assume that the magnetic clusters with individual net moments (i.e., AFM ordered clusters, with uncompensated spins) in a magnetically blocked state go to a magnetically frustrated state. This transition is due to dipolar-like interactions resulting in a cluster-glass-like state in our sample. Recall that the SG-like state may also find interparticle events, but the inter and intraparticle magnetic interactions cannot be distinguished with bulk-like magnetization experiments.

From the data of Fig. 2b, the relaxation time τ_0 of the magnetic moments for non-interacting single particles in a SPM regime can be calculated via an Arrhenius plot (see the Neél- Arrhenius law presented above; Eq. (1)).

Fig. 3 shows the resulting plot, where $\tau = 1/f_{AC}$ and T_{BF} is the temperature of the susceptibility peak for a given f_{AC}. The relaxation time determined by a linear fit of the experimental data is $\tau_0 = 3.7 \times 10^{-18}$ s. This value is not within the expected range (i.e., 10^{-9}–10^{-13} s) for non-interacting magnetic NPs, thus suggesting that the undoped NiO system at low temperatures cannot be reasonably described by this assumption (i.e., non-interacting particles).

We used dynamic scaling theory to determine if the sample shows a critical deceleration effect. This theory states that magnetic susceptibility varies as a power of the difference of the susceptibility peak temperature (T_{BF}) from the critical temperature (T_{sg}) at the critical transition temperature. Thus, the magnetic susceptibility diverges or vanishes at the critical point. The time scaling equation is

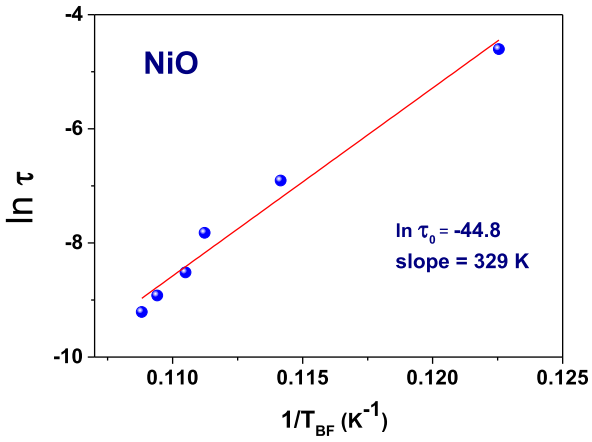

Fig. 3. ln τ *vs.* the reciprocal of T_{BF} for the undoped NiO sample. The solid line corresponds to a fit with the Arrhenius law.

given by:

$$\tau(f) = \tau^* \left[\frac{T_{sg}}{T_{BF} - T_{sg}} \right]^{zv}$$

here, the pre-factor τ^* is the relaxation time of an individual cluster or particle magnetic moments; the exponent (zv) describes the behavior of the relaxation time ($\tau(f)$) in the vicinity of the critical temperature and is called the *dynamic critical exponent*.

Fitting of the scaling law resulted in reasonable values for the critical exponent zv and the coherence time τ^* for the undoped NiO sample (see Fig. 4). The value of the critical exponent, zv = 8.55, is typical of spin-glass behavior (ranging 4–12 for spin-glass systems) [30]. The time $\tau^* = 2.06 \times 10^{-7}$ s is several orders larger than that for canonical spin glass systems ($\sim 10^{-13}$ s) [31] but agrees with the cluster spin glass system ($\sim 10^{-7}$–10^{-9} s) [30]. The higher spin flip time τ^* is due to atomic spin flip times or the flip times of superspin clusters. The spin glass transition is at $T_{sg} = 6.4$ K in close agreement with the experimental data.

To cite a related example, a spin-glass transition of 9–10 nm maghemite nanoparticles has also been reported by Martínez et al. [32]. The transition was attributed to random freezing of frustrated surface spins. Therefore, the spin-glass behavior in the NiO sample can be plausibly explained by surface spin-glass freezing.

M(H) measurements obtained for the undoped sample at 300 K and 2 K are shown in Fig. 5. None of the curves are saturated at the highest applied field (±7 T). The M(H) curve obtained at 300 K is a full straight line with a virtually null hysteresis, thus indicating that the NPs may be composed by, at least, two magnetic contributions: an AFM ordering related to both the shell and core and a PM portion that eventually exists in the shell. The M(H) loop obtained at 2 K reveals a robust hysteresis that also does not saturate even at a field of 7 T (see Mr and Hc values in Table 1), thus indicating the occurrence of ferromagnetic (FM) interactions or SG-like states in the NPs. Also, there is a slight tendency to saturate at the higher applied fields possibly reflecting a collective behavior at very low temperatures of NPs that carry net moments. The insert shows the abrupt change of the derivative of the descending magnetization, which indicates the behavior of non-coupled magnetic phases. It is worth note that the closure field is barely reached at the maximum applied field. The M(H) loops shown in Fig. 5 are like those obtained by others for NiO NPs [12,24,33–35].

Fig. 6 shows the M(T) curves for the Fe-doped (x = 0.02 and 0.04) NiO NPs. Similar M(T) curves were found for the x = 0.01 and 0.03 samples. Versus the undoped sample, the main difference is the apparent suppression of the broad peak attributed to the blocking of the AFM cores. One may consider that the iron doping strengthened the exchange interaction in the NPs (cores + shell), thus shifting the SPM blocking to higher temperatures. The positive derivative of the ZFC M(T) curve in the range ~100–300 K (see Fig. 6a insert) confirms this possibility because the maximum seems to occur above RT. This evidence is recurrent for the other samples heat treated at 600 °C. Remember that the crystallite size decreased as Fe dose increased as shown in Ref. [22]. Therefore, this observation is strongly correlated to an enhancement of the exchange interactions after Fe doping.

In contrast, the low temperature sharp peak is still present although the maxima position varies by ±1 K. The difference between the right-hand side of the ZFC peak and the FC curve along the same region is much smaller than the rest of the profile (see insert in Fig. 6b).

As considered for the undoped sample this peak could be attributed to the blocking or freezing of magnetic single domains, plausibly in the nanoparticle shell. For applied fields of 5000 Oe, this peak deviates to lower temperatures (curves not shown) with its maximum positioning at ~5 K.

AC characterization was also conducted for the x = 0.03 sample, and the results are shown in Fig. 7. The broad peak appears smoothed, and its mean position (i.e., 239(5) K) is slightly changed relatively to that found for the undoped sample (i.e., 232(4) K). In relative agreement with the DC curves [M(T)], the χ(T) curve flattening suggests that an additional part of the NPs is then magnetically blocked above RT, as an effect of the Fe-doping. Again, there is a group of low intensity peaks at 47 K, and the position of their maxima does not vary with the frequency. It is the same AFM transition earlier attributed to O_2. In contrast, the highest intensity peak,

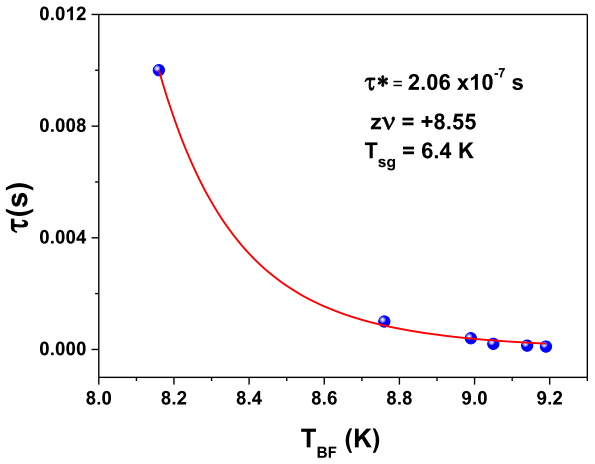

Fig. 4. Dynamic scaling law fit of the AC susceptibility peaks for the NiO sample.

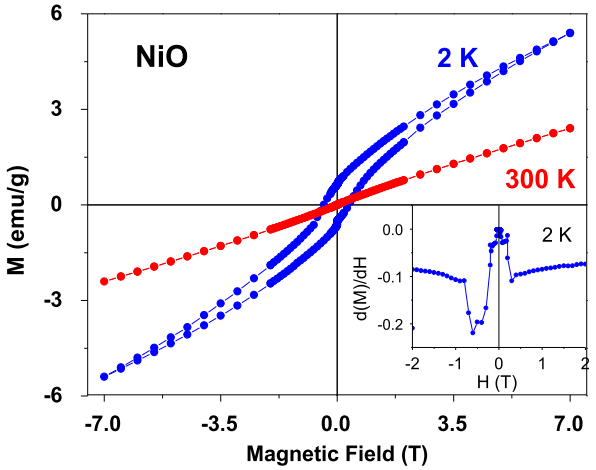

Fig. 5. M(H) curves obtained at RT and 2 K for the NiO sample. The insert is the derivative of the descending magnetization 2 K curve.

Table 1
Magnetic hysteresis parameters for the $Ni_{1-x}Fe_xO$ samples (2 K loops).

Sample (x)	T_{anneal} (°C)	Mr (emu/g)	Hc (Oe)
0.0	600	0.63	3769
0.01		0.09	1922
0.02		0.09	2110
0.03		0.02	1657
	400	0.02	1654
0.04	600	0.53	4340

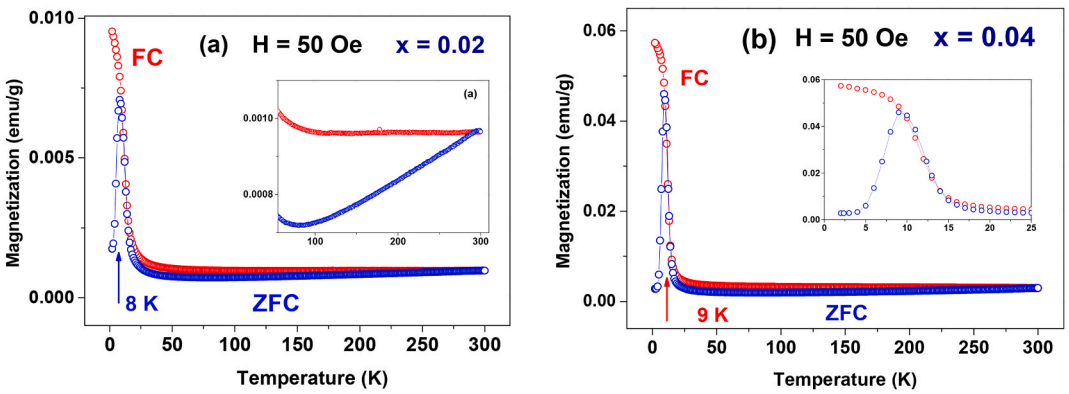

Fig. 6. M(T) curves (ZFC (blue) and FC (red) protocols) obtained with H = 50 Oe for the $Ni_{0.98}Fe_{0.02}O$ (the insert shows an expanded view of the 80–300 K range) (a) and $Ni_{0.96}Fe_{0.04}O$ (the insert shows an expanded view of the 2–25 K range) (b) samples.

identifiable at lowest temperature, changed its mean position and shifted collectively to higher temperatures. The peak reduced the variation range relatively to the maxima position versus the undoped sample (see Fig. 7b).

This shifting in temperature may be plausibly explained by the strengthening of the exchange interaction between the magnetic moments in the shell, whereas the narrowing of the peak set (i.e., individual linewidths and spacing between peaks) may be due to the reduction of the clusters size because the particle size decreases due to Fe-doping.

The C_1 *parameter* was also calculated for the $Ni_{0.97}Fe_{0.03}O$ sample to be 0.037(1), which suggests a SG-like transition at low temperatures (and plausibly also in the other Fe-doped samples).

An Arrhenius plot was also outlined from the above curves (see Fig. 8). In this case, $\tau_0 = 3 \times 10^{-30}$ s, which is several orders of magnitude smaller than the relaxation time found for the undoped sample. The inadequacy of a non-interacting particles model is more severe in this case or, in other words, doping with iron enhanced the interparticle interactions.

Fig. 9 shows the dynamic scaling law fit to the AC susceptibility peaks for the $Ni_{0.97}Fe_{0.03}O$ sample.

The parameters obtained from the fit were $\tau^* = 1.39 \times 10^{-9}$ s, zv = 6.8, and $T_{sg} = 9.4$ K. The relaxation time of the magnetic entities

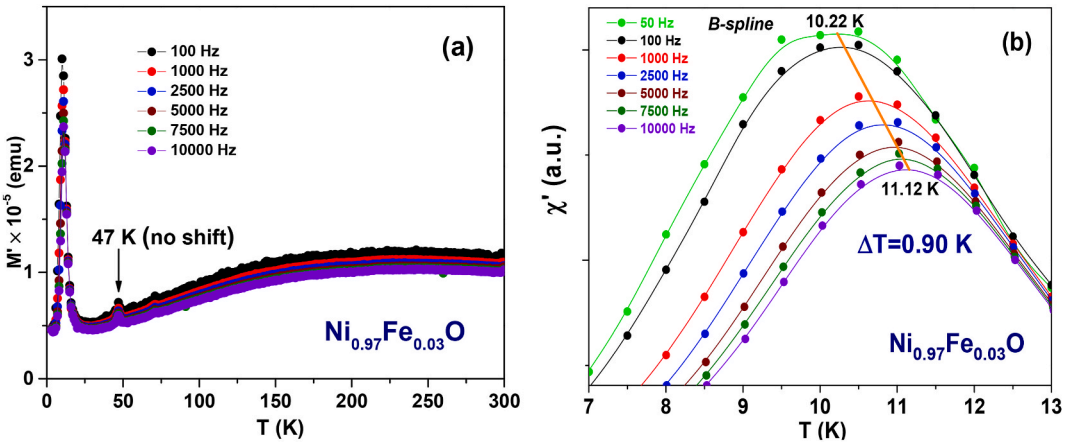

Fig. 7. χ(T) curves of the $Ni_{0.97}Fe_{0.03}O$ sample obtained for different frequencies, f_{AC} (a); expanded view of the 7–13 K range where the continuous solid lines are splines fits (b). The red dashed line connects the maxima (T_{BF}) of the 50 Hz and 10 kHz curves.

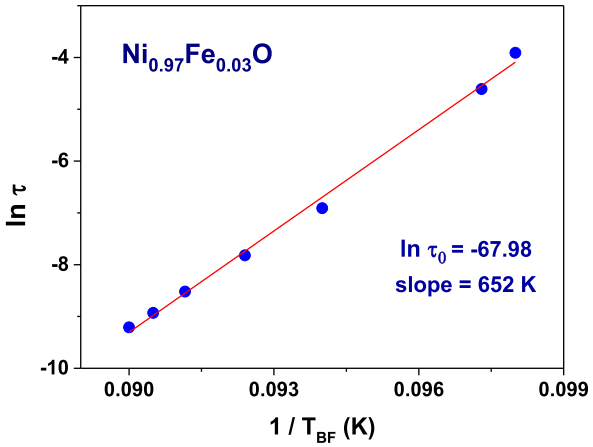

Fig. 8. ln τ *vs.* the reciprocal of T_{BF} (f), for the $Ni_{0.97}Fe_{0.03}O$ sample. The solid line corresponds to a fit using the Arrhenius law.

is within the expected range for a cluster spin glass system. Therefore, the critical exponent also corroborated the presence of a spin-glass magnetic phase. The higher transition temperature (T_{sg}) obtained for the Fe-doped NiO sample versus the undoped NiO sample may be related to a higher dipolar magnetic forces due to clusters with higher magnetic moments mostly due to the presence of Fe ions.

The M(H) measurements for the x = 0.02 and 0.04 samples are shown in Fig. 10.

At RT, the curves are again almost a straight line but have a faint S-shaped portion at low fields; thus, these data reproduce with subtle difference the M(H) curve for the undoped sample. As shown before, the M(H) curves obtained at 2 K revealed large hysteresis although the closure field is much lower for Fe-doped samples. Despite these differences, the FM- or SG-like phases are seen again.

Table 1 presents the main magnetic parameters of these and other samples, taken from the hystereses obtained at 2 K.

It is noteworthy that the magnetization at 7 T for the undoped sample is larger than the values found for the Fe-doped samples. Indeed, this follows the trend NiO > $Ni_{0.98}Fe_{0.04}O$ > $Ni_{0.97}Fe_{0.03}O$ > $Ni_{0.98}Fe_{0.02}O$ > $Ni_{0.99}Fe_{0.01}O$. The reduction of the maximum magnetization is the result of a complex combination of the Ni and Fe magnetic moments and the cationic vacancies originated by the Fe doping. The vacancies are consequence of the local electronic equilibrium, i.e., for each pair of Fe^{3+} introduced into the matrix (substituting two Ni cations), a "third" Ni^{2+} cation is just removed in order to locally equilibrate the negative (O^{2-}) and positive charges. Grain boundaries are formed if these point defects are numerous and sufficiently close, thus restricting the crystallite size. Although naturally existing in pure and stable $Ni_{1-\delta}O$ ($\delta \sim 5 \times 10^{-4}$), the fraction of Ni vacancies as well as the solubility limit for Fe doping of this catalyst depend on the synthesis process.

A good check for the existence of two magnetic phases should be done to study the exchange bias in the samples. However, the need to raise the temperature above RT before applying a magnetic field brings with it the risk that the NPs could evolve, thus changing their nature.

This is why a sample made of smaller NPs was prepared and characterized (i.e., the sample annealed at 400 °C). Its ^{57}Fe Mössbauer spectrum is shown in Supplementary Material and reveals a system fully in a SPM regime at RT. Therefore, it is reasonable to apply the field starting from RT down to 2 K (i.e., an FC condition) to investigate the exchange bias phenomenon.

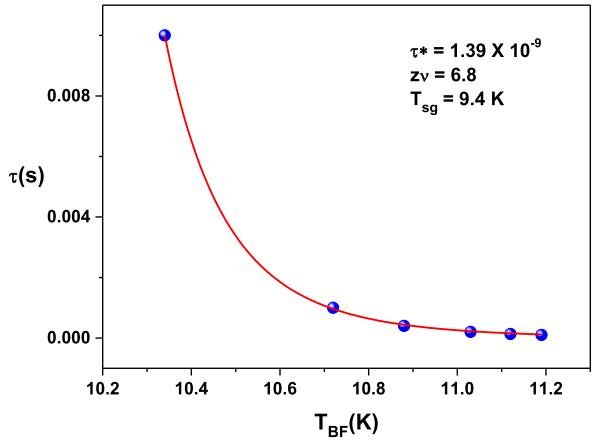

Fig. 9. Dynamic scaling law fit of the AC susceptibility peaks for the $Ni_{0.97}Fe_{0.03}O$ sample.

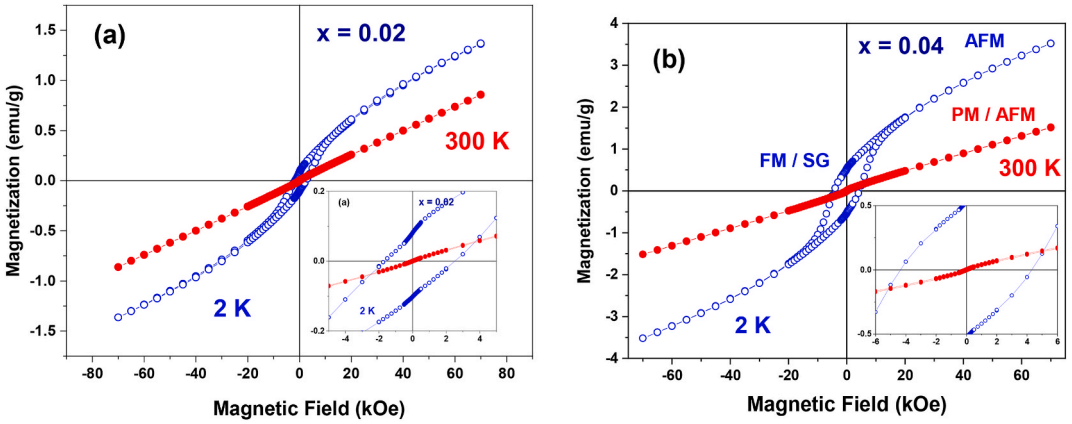

Fig. 10. M(H) curves obtained at RT and 2 K for the $Ni_{0.98}Fe_{0.02}O$ (a) and $Ni_{0.96}Fe_{0.04}O$ (b) samples. The inserts are expanded views of the hysteresis central parts.

The ZFC curve of this sample (see Fig. 11) shows the same apparent flat profile from 300 K down to ~50 K as revealed by the other Fe-doped samples though with a prominent shoulder in the low temperature peak (at ~20 K). In this respect, it repeats the behavior found for the undoped sample.

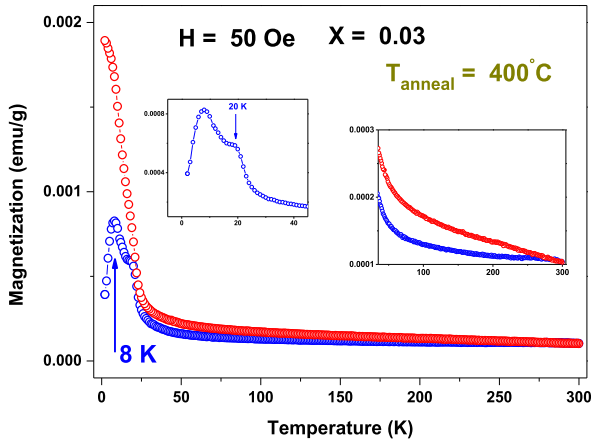

Fig. 11. M(T) curves - ZFC (blue) and FC (red) protocols obtained with H = 50 Oe for the $Ni_{0.97}Fe_{0.03}O$ sample. The inserts show expanded views of the 35–300 K range (right-hand side) and the 2–45 K range (left-hand side).

The insert in Fig. 11 (right-hand side) reveals the negative derivative of the ZFC curve in the range ~50–300 K, thus eventually having a maximum below 30 K and indicating that the SPM blocking of the system was shifted and spread out to lower temperatures. Here, this observation can be associated with a size effect (average diameter = 8.6 nm) on the NPs magnetic properties.

M(T) curves were also given for a sample annealed at a temperature between 400 °C and 600 °C (see Fig. 12). Consistent with the idea that the blocking temperature range depends on the NPsaverage size (average diameter = 12.2 nm, in this case), the low temperature maximum appears at ~250 K.

This illustrates how some magnetic properties can be tuned simply by controlling the NP size, which in this case can be done by heat treatment or Fe-doping.

The anisotropy constant calculated for these NPs (with $T = T_B$) resulted in K = 90,715 J/m^3, a value one order of magnitude higher than that calculated for the NiO NPs. This enhancement may be attributed to either the smaller size of these $Ni_{0.97}Fe_{0.03}O$ NPs in comparison with the NiO NPs or to the iron doping.

Fig. 13 shows the M(H) curves obtained for the x = 0.03 sample at 300 K and 2 K under ZFC and FC conditions. Robust loop shifting effects (along horizontal and vertical axes) are observed and can be attributed to two main contributions: exchange bias and/or a SG-like state in the sample. The exchange field (H_B = ~1300 Oe) reinforces the existence of two magnetic regions with a common interface such as in a core-shell NPs. The vertical and horizontal loop shifts are attributed to a minor loop effect (loop obtained in non-saturated regime) that often occurs in samples with a SG-like state in FC protocols [36].

4. Conclusions

$Ni_{1-x}Fe_xO$ monophasic nanoparticles synthesized by the lyophilization method were characterized by magnetization techniques, and the results are consistent with the core-shell model regularly employed to describe undoped NiO nanoparticles.

Above RT, the shell and core of the undoped NiO nanoparticles are respectively in a PM state and SPM regime, whereas the core is progressively blocked magnetically decreasing the sample temperature in the range 50–300 K. Below 50 K, AFM clusters with a net magnetic moment start to grow and block in the shell. Eventually, they freeze below 10 K leading the undoped and Fe-doped NiO NPs to a cluster-glass-like state. The cluster-glass-like state occurs by dipolar magnetic interactions of NiO NPs after they enter in a magnetically blocked state.

The Fe-doped NiO nanoparticles undergo the same transitions although triggered at different temperatures due to an enhancement of magnetic exchange interaction caused by the Fe doping. Particularly, the anisotropy constant of the $Ni_{0.97}Fe_{0.03}O$ sample revealed to be significantly larger than that of the undoped sample.

CRediT authorship contribution statement

Alex Soares de Brito: Data curation, Investigation, Methodology, Software. **Marlon Ivan Valerio-Cuadros:** Data curation, Investigation, Methodology, Software. **Lilian Felipe Silva Tupan:** Data curation, Investigation, Methodology, Software. **Aline Alves Oliveira:** Data curation, Investigation, Methodology, Software. **Reginaldo Barco:** Formal analysis, Investigation, Methodology, Resources. **Flávio Francisco Ivashita:** Formal analysis, Investigation, Methodology, Resources. **Edson Caetano Passamani:** Conceptualization, Data curation, Writing – review & editing. **José Humberto de Araújo:** Conceptualization, Writing – review & editing. **Marco Antonio Morales Torres:** Conceptualization, Data curation, Writing – review & editing. **Andrea Paesano:** Conceptualization, Project administration, Supervision, Writing – original draft, Writing – review & editing.

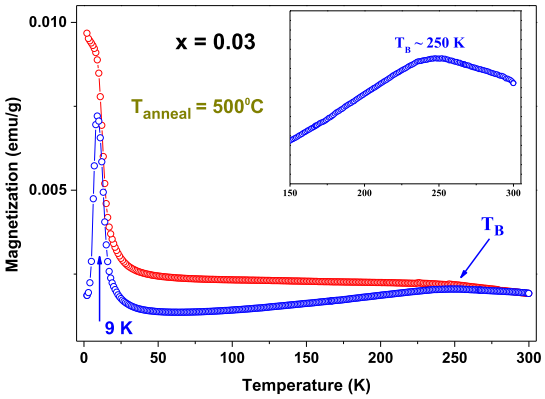

Fig. 12. M(T) curves - ZFC (blue) and FC (red) protocols obtained with H = 50 Oe for the $Ni_{0.97}Fe_{0.03}O$ sample annealed at 500 °C. The insert shows an expanded view of the 150–300 K range.

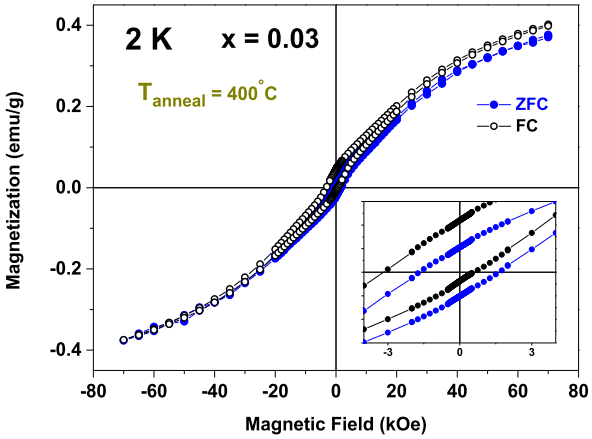

Fig. 13. M(H) curves obtained at 2 K for the $Ni_{0.97}Fe_{0.03}O$ sample annealed at 400 °C, in ZFC (blue curve) and FC (black curve) conditions. The insert is an expanded view of the hysteresis central parts.

Declaration of competing interest

The authors declare that they have no known competing financial interests or personal relationships that could have appeared to influence the work reported in this paper.

Acknowledgements

The authors thank CNPq/Fundação Araucária (Grant PRONEX 46824) for financial support. Marlon I. Valerio-Cuadros thanks the "Incorporación de Investigadores program" CONCYTEC–FONDECYT. UNMSM (Contrat No. 12-2019 – FONDECYT – BM – INC – INV.) for supporting his work at the University of San Marcos. Edson C. Passamani is grateful for financial support from Fundação de Amparo à Pesquisa e Inovação do Espírito Santo (FAPES: TO-975/2022 and TO-496/2021) and Conselho Nacional de Desenvolvimento Científico e Tecnológico (CNPq).

Appendix A. Supplementary data

Supplementary data to this article can be found online at https://doi.org/10.1016/j.heliyon.2023.e22876.

References

[1] N. Rinaldi-Montes, P. Gorria, D. Martínez-Blanco, A.B. Fuertes, L.F. Barquín, I. Puente-Orench, J.A. Blanco, Scrutinizing the role of size reduction on the exchange bias and dynamic magnetic behavior in NiO nanoparticles, Nanotechnology 26 (2015), 305705, https://doi.org/10.1088/0957-4484/26/30/305705.
[2] M. Tadic, D. Nikolic, M. Panjan, G.R. Blake, Magnetic properties of NiO (nickel oxide) nanoparticles: blocking temperature and Neel temperature, J. Alloys Compd. 647 (2015) 1061–1068, https://doi.org/10.1016/j.jallcom.2015.06.027.
[3] D. Nikolić, M. Panjan, G.R. Blake, M. Tadić, Annealing-dependent structural and magnetic properties of nickel oxide (NiO) nanoparticles in a silica matrix, J. Eur. Ceram. Soc. 35 (2015) 3843–3852, https://doi.org/10.1016/j.jeurceramsoc.2015.06.024.
[4] E. Winkler, R.D. Zysler, M.V. Mansilla, D. Fiorani, Surface anisotropy effects in NiO nanoparticles, Phys. Rev. B 72 (2005), 132409, https://doi.org/10.1103/PhysRevB.72.132409.
[5] L. Néel, Théorie du traînage magnétique des ferromagnétiques en grains fins avec application aux terres cuites, Ann. Geophys.(149AD) 99–136. https://hal.science/hal-03070532 (accessed February 6, 2023).
[6] L. Néel, Anisotropie magnétique superficielle et surstructures d'orientation, J. Phys. Radium 15 (1954) 225–239, https://doi.org/10.1051/jphysrad:01954001504022500.
[7] R.H. Kodama, S.A. Makhlouf, A.E. Berkowitz, Finite size effects in antiferromagnetic NiO nanoparticles, Phys. Rev. Lett. 79 (1997) 1393–1396, https://doi.org/10.1103/PhysRevLett.79.1393.
[8] R.H. Kodama, Magnetic nanoparticles, J. Magn. Magn Mater. 200 (1999) 359–372, https://doi.org/10.1016/S0304-8853(99)00347-9.
[9] A.K. Mishra, S. Bandyopadhyay, D. Das, Structural and magnetic properties of pristine and Fe-doped NiO nanoparticles synthesized by the co-precipitation method, Mater. Res. Bull. 47 (2012) 2288–2293, https://doi.org/10.1016/j.materresbull.2012.05.046.
[10] S.A. Makhlouf, F.T. Parker, F.E. Spada, A.E. Berkowitz, Magnetic anomalies in NiO nanoparticles, J. Appl. Phys. 81 (1997) 5561–5563, https://doi.org/10.1063/1.364661.
[11] S.D. Tiwari, K.P. Rajeev, Signatures of spin-glass freezing in NiO nanoparticles, Phys. Rev. B 72 (2005), 104433, https://doi.org/10.1103/PhysRevB.72.104433.
[12] K.O. Moura, R.J.S. Lima, A.A. Coelho, E.A. Souza-Junior, J.G.S. Duque, C.T. Meneses, Tuning the surface anisotropy in Fe-doped NiO nanoparticles, Nanoscale 6 (2014) 352–357, https://doi.org/10.1039/C3NR04926D.
[13] F. Bødker, M.F. Hansen, C. Bender Koch, S. Mørup, Particle interaction effects in antiferromagnetic NiO nanoparticles, J. Magn. Magn Mater. 221 (2000) 32–36, https://doi.org/10.1016/S0304-8853(00)00392-9.
[14] E. Winkler, R.D. Zysler, M. Vasquez Mansilla, D. Fiorani, D. Rinaldi, M. Vasilakaki, K.N. Trohidou, Surface spin-glass freezing in interacting core–shell NiO nanoparticles, Nanotechnology 19 (2008), 185702, https://doi.org/10.1088/0957-4484/19/18/185702.

[15] A.O. de Souza, F.F. Ivashita, V. Biondo, A. Paesano, D.H. Mosca, Structural and magnetic properties of iron doped ZrO_2, J. Alloys Compd. 680 (2016) 701–710, https://doi.org/10.1016/j.jallcom.2016.04.170.
[16] A.A. Oliveira, M.I. Valerio-Cuadros, L.F.S. Tupan, F.F. Ivashita, A. Paesano, Size-effect on the optical behavior of Fe-doped CuO nanoparticles synthesized by a freeze-drying process, Mater. Lett. 229 (2018) 327–330, https://doi.org/10.1016/j.matlet.2018.07.009.
[17] J. Wang, J. Cai, Y.-H. Lin, C.-W. Nan, Room-temperature ferromagnetism observed in Fe-doped NiO, Appl. Phys. Lett. 87 (2005), 202501, https://doi.org/10.1063/1.2130532.
[18] A.P. Douvalis, L. Jankovic, T. Bakas, The origin of ferromagnetism in 57Fe-doped NiO, J. Phys. Condens. Matter 19 (2007), 436203, https://doi.org/10.1088/0953-8984/19/43/436203.
[19] A.C. Gandhi, S.Y. Wu, Thermal annealing induced enhancement of room temperature magnetic memory effect in Fe-doped NiO nanoparticles, AIP Adv. 10 (2020), 015211, https://doi.org/10.1063/1.5129785.
[20] S. Philip Raja, C. Venkateswaran, Investigation of magnetic behaviour of Ni–Fe–O prepared by the solid state method, J. Phys. D Appl. Phys. 42 (2009), 145001, https://doi.org/10.1088/0022-3727/42/14/145001.
[21] J.H. He, S.L. Yuan, Y.S. Yin, Z.M. Tian, P. Li, Y.Q. Wang, K.L. Liu, C.H. Wang, Exchange bias and the origin of room-temperature ferromagnetism in Fe-doped NiO bulk samples, J. Appl. Phys. 103 (2008), 023906, https://doi.org/10.1063/1.2832437.
[22] A.S. de Brito, A.A. Oliveira, M.I. Valerio-Cuadros, L.F. da S. Tupan, C.C.P. Cid, P.D. Macruz, R.P. Nippes, V.S. Zanuto, O.A.A. dos Santos, A. Paesano, Photocatalytic properties of Ni1-xFexO nanoparticles synthesized by a freeze-drying process, Mater. Chem. Phys. 299 (2023), 127488, https://doi.org/10.1016/j.matchemphys.2023.127488.
[23] M.P. Proenca, C.T. Sousa, A.M. Pereira, P.B. Tavares, J. Ventura, M. Vazquez, J.P. Araujo, Size and surface effects on the magnetic properties of NiO nanoparticles, Phys. Chem. Chem. Phys. 13 (2011) 9561, https://doi.org/10.1039/c1cp00036e.
[24] S. Thota, J. Kumar, Sol–gel synthesis and anomalous magnetic behaviour of NiO nanoparticles, J. Phys. Chem. Solid. 68 (2007) 1951–1964, https://doi.org/10.1016/j.jpcs.2007.06.010.
[25] G.F. Goya, H.R. Rechenberg, J.Z. Jiang, Magnetic irreversibility and relaxation in $CuFe_2O_4$ nanoparticles, J. Magn. Magn Mater. 218 (2000) 221–228, https://doi.org/10.1016/S0304-8853(00)00339-5.
[26] M. Bałanda, AC susceptibility studies of phase transitions and magnetic relaxation: conventional, molecular and low-dimensional magnets, Acta Phys. Pol., A 124 (2013) 964–976, https://doi.org/10.12693/APhysPolA.124.964.
[27] J.A. Mydosh, Spin Glasses, CRC Press, 2014, https://doi.org/10.1201/9781482295191.
[28] J.L. Dormann, D. Fiorani, E. Tronc, Magnetic Relaxation in Fine-Particle Systems, J. Wiley, 1997, pp. 283–494, https://doi.org/10.1002/9780470141571.ch4.
[29] M. Vrankić, A. Šarić, S. Bosnar, D. Pajić, J. Dragović, A. Altomare, A. Falcicchio, J. Popović, M. Jurić, M. Petravić, I.J. Badovinac, G. Dražić, Magnetic oxygen stored in quasi-1D form within $BaAl_2O_4$ lattice, Sci. Rep. 9 (2019), 15158, https://doi.org/10.1038/s41598-019-51653-4.
[30] J. Souletie, J.L. Tholence, Critical slowing down in spin glasses and other glasses: fulcher versus power law, Phys. Rev. B 32 (1985) 516–519, https://doi.org/10.1103/PhysRevB.32.516.
[31] P.C. Hohenberg, B.I. Halperin, Theory of dynamic critical phenomena, Rev. Mod. Phys. 49 (1977) 435–479, https://doi.org/10.1103/RevModPhys.49.435.
[32] B. Martínez, X. Obradors, Ll Balcells, A. Rouanet, C. Monty, Low temperature surface spin-glass transition in γ-Fe_2O_3 nanoparticles, Phys. Rev. Lett. 80 (1998) 181–184, https://doi.org/10.1103/PhysRevLett.80.181.
[33] N. Rinaldi-Montes, P. Gorria, D. Martínez-Blanco, A.B. Fuertes, L. Fernández Barquín, J. Rodríguez Fernández, I. de Pedro, M.L. Fdez-Gubieda, J. Alonso, L. Olivi, G. Aquilanti, J.A. Blanco, Interplay between microstructure and magnetism in NiO nanoparticles: breakdown of the antiferromagnetic order, Nanoscale 6 (2014) 457–465, https://doi.org/10.1039/c3nr03961g.
[34] M. Arif, A. Sanger, M. Shkir, A. Singh, R.S. Katiyar, Influence of interparticle interaction on the structural, optical and magnetic properties of NiO nanoparticles, Phys. B Condens. Matter 552 (2019) 88–95, https://doi.org/10.1016/j.physb.2018.09.023.
[35] F.H. Aragón, P.E.N. de Souza, J.A.H. Coaquira, P. Hidalgo, D. Gouvêa, Spin-glass-like behavior of uncompensated surface spins in NiO nanoparticulated powder, Phys. B Condens. Matter 407 (2012) 2601–2605, https://doi.org/10.1016/j.physb.2012.04.003.
[36] E.C. Passamani, C. Larica, C. Marques, A.Y. Takeuchi, J.R. Proveti, E. Favre-Nicolin, Large vertical loop shifts in mechanically synthesized $(Mn,Fe)_2O_3$−t nanograins, J. Magn. Magn Mater. 314 (2007) 21–29, https://doi.org/10.1016/j.jmmm.2007.02.008.